# Fabrication and properties of epitaxial ferroelectric heterostructures with ($SrRuO_3$) isotropic metallic oxide electrodes

C. B. Eom, R. B. Van Dover, Julia M. Phillips, D. J. Werder, J. H. Marshall, C. H. Chen, R. J. Cava, and R. M. Fleming
*AT&T Bell Laboratories, Murray Hill, New Jersey 07974*

D. K. Fork
*Xerox Palo Alto Research Center, Palo Alto, California 94304*

(Received 27 May 1993; accepted for publication 23 August 1993)

Epitaxial ferroelectric $SrRuO_3/Pb(Zr_{0.52}Ti_{0.48})O_3/SrRuO_3$ heterostructures have been fabricated employing isotropic metallic oxide electrodes on (100) $SrTiO_3$ and (100) Si with an yttria stabilized zirconia buffer layer. The structures have been grown *in situ* by 90° off-axis sputtering, which allows the growth of uniform stoichiometric films over large areas with excellent step coverage. X-ray diffraction, Rutherford backscattering spectroscopy, and cross-sectional transmission electron microscopy reveal high crystalline quality and coherent interfaces. They exhibit superior fatigue characteristics over those made with metal electrodes, showing little degradation over $10^{10}$ cycles, with a large remnant polarization.

Ferroelectrics have excellent potential for both dynamic and permanent data storage in digital memory systems.[1] Conventionally, polycrystalline ferroelectric thin films are grown on Pt base electrodes. The high angle grain boundaries which occur in the ferroelectric thin film layer are detrimental to device performance, causing aging and fatigue due to charge segregation and decay. Furthermore, the nonideal interfaces between ferroelectric layers and electrodes leads to degraded performance.[2] Ramesh *et al.* reported that epitaxial thin film heterostructures of ferroelectric materials and cuprate superconductor electrodes grown by laser ablation have outstanding fatigue properties.[2,3] Unfortunately, the cuprate superconductors are neither isotropic conductors nor fully chemically and thermally stable, which puts constraints on their processing and usage. Furthermore, high $T_c$ superconducting thin films typically have relatively poor crystalline quality and rough surfaces. These drawbacks may limit the applications of cuprate electrodes for nonvolatile memory applications.

We recently grew single crystal epitaxial thin films of the isotropic metallic oxide $SrRuO_3$ on miscut (100) $SrTiO_3$.[4] $SrRuO_3$ is a pseudocubic perovskite, with a pseudocubic lattice parameter of 3.93 Å.[5,6] [Note: the *a*- and *c*-lattice parameters of $Pb(Zr_{0.52}Ti_{0.48})O_3$ (PZT) are 4.036 and 4.146 Å, respectively.] The lattice mismatch of $SrRuO_3$ and the ferroelectric PZT on the {001} surface is fairly small ($\sim$2.7%), which allows us to grow high quality epitaxial ferroelectric heterostructures with $SrRuO_3$ electrodes. Unlike most oxide superconductors, $SrRuO_3$ is stable up to 1200 K in oxidizing or inert gas atmospheres.[7] The resistivities of $SrRuO_3$ films are isotropic and low ($\sim 340\ \mu\Omega$ cm at room temperature), and the temperature dependence ($d\rho/dT$) shows good metallic behavior, which is important for electrode applications. These films exhibit pure $\{110\}^{\dagger}$ texture normal to the substrate. [† defines Miller indices on an orthorhombic unit cell, therefore (100) texture based on a pseudocubic unit cell.] The films are "single domain" with in-plane epitaxial arrangement of $SrRuO_3[\bar{1}10] \| SrTiO_3[010]$ and $SrRuO_3[001] \| SrTiO_3[001]$. The surfaces are extremely smooth [root-mean-square surface roughness of $6.9 \pm 0.2$ Å], which is important for multilayered device fabrication. The growth temperature for $SrRuO_3$ thin films is lower than that used for cuprate superconductors, which is desirable to minimize interdiffusion. All of these observations suggest that $SrRuO_3$ might be an ideal electrode material for epitaxial ferroelectric device structures.

In this letter, we present results on epitaxial ferroelectric heterostructures with $SrRuO_3$ electrodes on (100) $SrTiO_3$ and Si with an yttria stabilized zirconia (YSZ) buffer layer.[8] These heterostructures ($SrRuO_3$/PZT/$SrRuO_3$) were grown *in situ* by 90° off-axis sputtering,[9–12] which produces large area (2 in.×2 in.) films whose composition is nearly identical to the target without substrate block rotation. This technique allows very good coverage, which is important in fabricating ferroelectric devices. The substrate block temperature was held at 680 °C during $SrRuO_3$ and 530 °C during PZT deposition.

First, the optimum conditions for growing epitaxial PZT layers were determined. The composition of the films was measured on 1000-Å-thick films on MgO(100) with Rutherford backscattering spetroscopy and found to be stoichiometric within experimental error. There was no indication of interdiffusion at the interface The single layer on (100)$SrTiO_3$ shows pure *c*-axis orientation. Atomic force microscopy reveals the root-mean-square surface roughness of the films to be 7 Å.

Next, we made and characterized two types of bilayers on (100)$SrTiO_3$ substrates. A PZT(1000 Å) layer on a $SrRuO_3$(1000 Å) layer exhibited only (00*l*) peaks of PZT and (*hh*0) peaks of $SrRuO_3$, showing good epitaxy of the ferroelectric layer on the $SrRuO_3$ bottom electrode [see Fig. 1(a)]. The rocking curve width [full width at half-maximum (FWHM)] of the (002) PZT peak was 0.35°, and the $\chi_{min}$ along ⟨100⟩ was 30%. In a $SrRuO_3$(1000 Å) layer on a PZT(1000 Å) film. (*hh*0) peaks of $SrRuO_3$ and (00*l*) peaks of PZT appears again showing good epitaxy of



Downloaded 03 Nov 2002 to 128.104.185.74. Redistribution subject to AIP license or copyright, see http://ojps.aip.org/aplo/aplcr.jsp

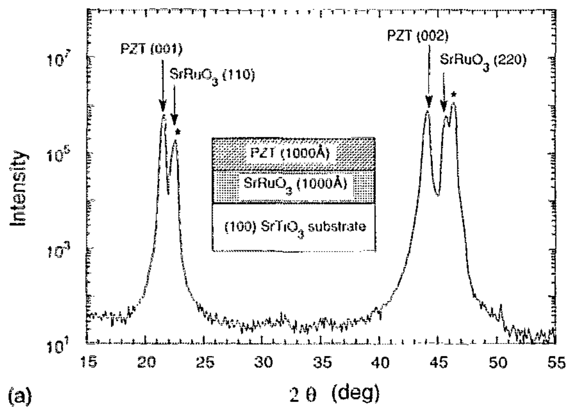


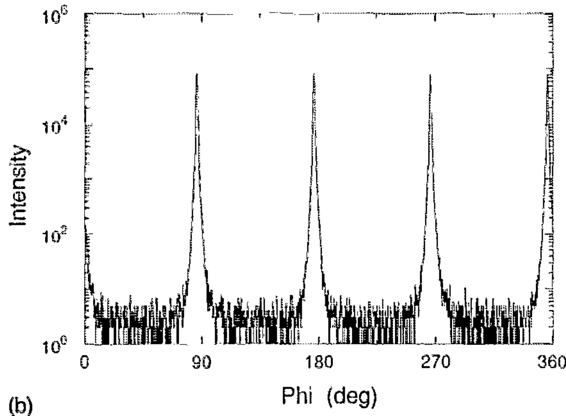


FIG. 1. (a) X-ray diffraction $\theta$-$2\theta$ scan of a PZT/$SrRuO_3$ heterostructure on (100) $SrTiO_3$ showing (001) PZT and (110) $SrRuO_3$ oriented films. $SrTiO_3$ peaks are marked (*). (b) Off-axis x-ray $\phi$ scan of the PZT (110) peak for a PZT/$SrRuO_3$ heterostructure on (100) $SrTiO_3$ showing a in-plane epitaxy.

the $SrRuO_3$ top electrode on the ferroelectric layer. The rocking curve width (FWHM) of the (220) $SrRuO_3$ peak was 0.55°.

Figure 1(b) shows a $\phi$ scan (azimuthal scan) of the PZT(110) reflection for the PZT/$SrRuO_3$ heterostructure. The significant intensities only at $\phi=0°$, 90°, 180°, and 270°, clearly indicate the inplane epitaxial arrangement of PZT[100]|| $SrRuO_3$[$\bar{1}$10]|| $SrTiO_3$[010], and PZT[100]|| $SrRuO_3$[001]|| $SrTiO_3$[001] without misoriented PZT grains.

Capacitor device structures were fabricated on (100) $SrTiO_3$ and (100) Si with a YSZ buffer layer as shown in Fig. 2(a). The structure consists of a 2000-Å-thick $SrRuO_3$ bottom electrode with 5000-Å-thick PZT and 800-Å-thick $SrRuO_3$ layers deposited through a 100-$\mu$m-thick Si shadow mask. Finally, a 500-Å layer of Au was deposited by dc magnetron sputtering at room temperature for wire bonding. These quatralayers were patterned using standard photolithographic processing and ion milling to form a set of 200 $\mu$m$\times$200 $\mu$m square capacitors.

Figure 3(a) shows a cross-sectional transmission electron micrograph (TEM) of the capacitor structure on (100) $SrTiO_3$ along the ⟨100⟩ zone axis. The $SrRuO_3$ bottom electrode is single domain, promoting growth of a high quality PZT layer on top. The $SrRuO_3$ top electrode is not single domain, displaying (110) epitaxy normal to the substrate, but with two in-plane orientations. Figures 3(b) and 3(c) are high magnification images of the substrate/bottom electrode and PZT/bottom electrode interfaces, respectively. In spite of the single domain bottom electrode, low angle domain boundaries can be seen in the PZT layer due to columnar growth, as indicated by arrows.

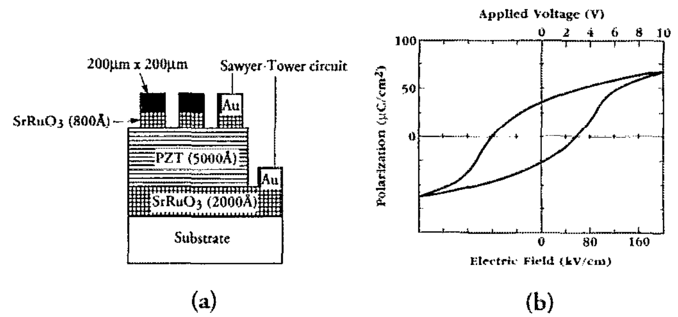


FIG. 2. (a) Schematic illustration of the capacitor test structure used. (b) A typical ferroelectric hysteresis loop obtained from $SrRuO_3$/PZT/$SrRuO_3$ heterostructures at room temperature.

The electrical properties of the capacitors were examined using a conventional Sawyer–Tower circuit.[13] The ferroelectric hysteresis is illustrated in Fig. 2(b). For the devices on $SrTiO_3$ the remnance was 27 $\mu C/cm^2$, very close to the bulk value. The corresponding coercive field and coercive voltage were about 70 kV/cm and 3.5 V, respectively. The shape of the ferroelectric hysteresis loops was independent of frequency in the range 10–100 kHz. The capacitors on YSZ buffered Si showed lower remnant polarization (10.5 $\mu C/cm^2$) than those on $SrTiO_3$. We believe that this is mainly due to the $SrRuO_3$ layer growing with $(110)^{\dagger\dagger}$ orientation on the YSZ buffered Si. (†† defines Miller indices based on an pseudocubic perovskite subcell.) The PZT layer on the $(110)^{\dagger\dagger}$ $SrRuO_3$ layer exhibited (110) orientation by x-ray diffraction, which is not its favorable polarization direction. We have recently been able to grow a $(100)^{\dagger\dagger}$ $SrRuO_3$ layer on both $BaZrO_3$/MgO and $CeO_2$/YSZ double buffer layers on Si, which will allow us to grow $c$-axis oriented PZT on top of them.[14]

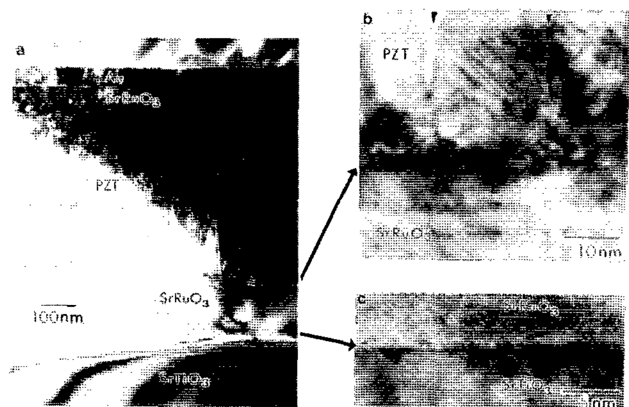


FIG. 3. (a) Low magnification cross-sectional TEM micrograph of a Au/$SrRuO_3$/PZT/$SrRuO_3$ heterostructure on (100) $SrTiO_3$. High magnification cross-sectional TEM images showing (b) the substrate/$SrRuO_3$ interface, and (c) $SrRuO_3$ bottom electrode/PZT interface.


Downloaded 03 Nov 2002 to 128.104.185.74. Redistribution subject to AIP license or copyright, see http://ojps.aip.org/aplo/aplcr.jsp

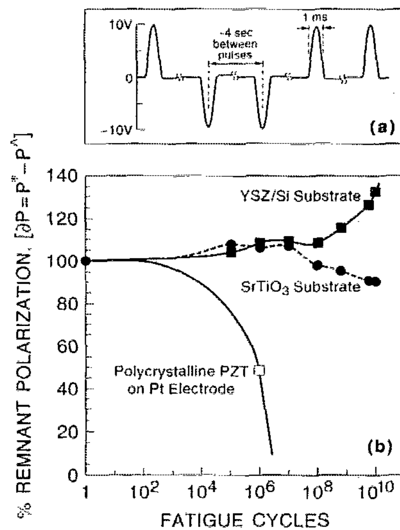


FIG. 4. (a) The pulse train used to measure the effective read cycle discrimination $\partial P$. (b) Remnant polarization $\partial P$ vs number of fatigue cycles at 10 V for the $SrRuO_3/PZT/SrRuO_3/SrTiO_3$ and $SrRuO_3/PZT/SrRuO_3/YSZ/Si$ structures, compared with data for a typical polycrystalline ferroelectric layer on a Pt base electrode. The solid line is a guide to the eye based on behavior reported in the literature (Ref. 1).

Pulsed hysteresis measurements for fatigue tests were made using a Sawyer–Tower circuit with the wave form shown in Fig. 4(a). A quiescent time of 4 s between pulses allowed full relaxation of any transient effects in the PZT.[15] The pulses were formed using an HP 8112 Å pulse generator under computer control and had a Gaussian profile with a 1.5-ms width and 1-ms transitions. The response was measured digitally with an HP 7090 digitizer and corrected for parasitic effects. The samples were stressed by bursts of 17.2-ms square wave using $V_{max}=10\ V_{p-p}$ (200 $kV_{p-p}$/cm), comparable to the patterns commonly employed in simple fatigue tests.[2] Figure 4 shows the normalized remnant polarization, $\partial P$ vs number of fatigue cycles, for $SrRuO_3/PZT/SrRuO_3$ capacitors on both $SrTiO_3$ and YSZ buffered Si . The data of Fig. 4(b) represent the effective read-cycle discrimination between a written "1" and "0" (sample pulsed to $-V_{max}$); in conventional notation $\partial P = P^* - \hat{P}$ .

For a polycrystalline PZT layer on a Pt electrode,[1] the remnant polarization drops to 50% of its initial value after $10^6$ cycles, but for epitaxial PZT layers between $SrRuO_3$ electrodes, the remnant polarization remains virtually unchanged from its initial value. After $10^{10}$ cycles, the capacitors on $SrTiO_3$ show only a 10% decay of remnant polarization. However, $\partial P$ increases monotonically after $10^8$ cycles in the capacitors on YSZ buffer layered Si substrates. This improvement in fatigue behavior is attributed to improved electrode–ferroelectric interfaces, and the absence of high angle grain boundaries in the PZT layers, as observed in epitaxial ferroelectric layers between YBCO electrodes[2] and other metallic oxide electrodes such as $RuO_x$ and $La_{0.5}Sr_{0.5}CoO_3$.[16,17]

Epitaxial ferroelectric heterostructures of $SrRuO_3$/$Pb(Zr_{0.52}Ti_{0.48})O_3$ (PZT)/$SrRuO_3$ can be grown on (100) $SrTiO_3$ and (100)Si with a YSZ buffer layer *in situ* by 90° off-axis sputtering. This technique has allowed us to grow uniform stoichiometric films over a large area with very good step coverage, offering a very promising technique for fabricating ferroelectric devices. The single crystal $SrRuO_3$ bottom electrode has high crystalline quality and a smooth surface, promoting growth of high quality PZT. The thermal and chemical stability of the electrode material permit flexibility in the device fabrication processes, as well as long-term reliability of the devices at high temperature and in corrosive environments. Fatigue characteristics of the ferroelectric heterostructures with $SrRuO_3$ electrodes are far superior to those obtained with polycrystalline ferroelectric layers on Pt electrodes. These epitaxial heterostructures of ferroelectric/isotropic metallic oxide electrodes look promising for use as nonvolatile memory devices.

We would like to thank J. T. Evans (Radiant Technologies), E. S. Hellman, A. Kussmaul, D. G. Schlom, E. H. Hartford, K. Short, and D. W. Murphy for helpful discussions.

[1] J. F. Scott and C. A. Paz de Araujo, Science **246**, 1400 (1989).
[2] R. Ramesh, W. K. Chan, B. Wilkens, H. Gilchrist, T. Sands, J. M. Tarascon, V. G. Keramidas, D. K. Fork, J. Lee, and A. Safari, Appl. Phys. Lett. **61** 1537 (1992).
[3] R. Ramesh, A. Inam, W. K. Chan, B. Wilkens, K. Myers, K. Remschnig, D. L. Hart, and J. M. Tarascon, Science **252**, 944 (1991).
[4] C. B. Eom, R. J. Cava, R. M. Fleming, Julia M. Phillips, R. B. van Dover, J. H. Marshall, J. W. P. Hsu, J. J. Krajewski, and W. F. Peck, Jr., Science **258**, 1766 (1993).
[5] P. R. Van Loan, Ceram. Bull. **51**, 231 (1972).
[6] R. J. Bouchard and J. L. Gillson, Mater. Res. Bull **7**, 873 (1972).
[7] W. Bensch, H. W. Schmalle, and A. Reller, Solid State Ionics, Diffusion Reactions **43**, 171 (1990).
[8] D. K. Fork, D. B. Fener, R. W. Barton, J. M. Philips, G. A. N. Connell, J. B. Boyce, and T. H. Geballe, Appl. Phys. Lett. **57**, 1161 (1990).
[9] C. B. Eom, J. Z. Sun, K. Yamamoto, A. F. Marshall, K. E. Luther, S. S. Laderman, and T. H. Geballe, Appl. Phys. Lett. **55**, 595 (1989).
[10] C. B. Eom, J. Z. Sun, S. K. Streiffer, A. F. Marshall, K. Yamamoto, B. M. Lairson, S. M. Anlage, J. C. Bravman, T. H. Geballe, S. S. Laderman, and R. C. Taber, Physica C **171**, 351 (1990).
[11] J. D. Klein and A. Yen, Mater. Res. Soc. Symp. Proc. **243**, 167 (1992).
[12] C. B. Eom, A. F. Marshall, J.-M. Triscone, B. Wilkens, S. S. Laderman, and T. H. Geballe, Science **251**, 780 (1991).
[13] C. B. Sawyer and C. H. Tower, Phys. Rev. **35**, 269 (1930).
[14] C. B. Eom, J. M. Phillips, and J. H. Marshall (unpublished).
[15] J. T. Evans (private communication).
[16] S. D. Berstein, T. Y. Wong, Y. Kisler, and R. W. Tustison, J. Mater. Res. **8**, 12 (1993).
[17] J. T. Cheung and R. R. Neurgaonkar, in Proceedings of the 1993 Materials Research Society Spring Meeting, San Francisco, CA, April 1993; J. T. Cheung, P. E. D. Morgan, D. H. Lowndes, X-Y Zheng, and J. Breen, Appl. Phys. Lett. **62**, 2045 (1993).



Downloaded 03 Nov 2002 to 128.104.185.74. Redistribution subject to AIP license or copyright, see http://ojps.aip.org/aplo/aplcr.jsp